Properties of InN layers grown on 6H–SiC(0001) by plasma-assisted molecular beam epitaxy

Tommy Ive,[a] Oliver Brandt, Manfred Ramsteiner, Manfred Giehler, Helmar Kostial, and Klaus H. Ploog
Paul-Drude-Institut für Festkörperelektronik, Hausvogteiplatz 5-7, D-10117 Berlin, Germany

(Received 5 August 2003; accepted 14 January 2004)

We study the impact of different buffer layers and growth conditions on the properties of InN layers grown on 6H–SiC(0001) by plasma-assisted molecular beam epitaxy. Both GaN and AlN buffer layers result in a significant improvement of the structural quality compared to InN layers grown directly on the SiC substrate. However, to obtain layers exhibiting a high structural integrity, smooth surface morphology, high mobility and strong band-to-band photoluminescence, contradicting growth conditions are found to be required. Furthermore, since InN(0001) dissociates already at temperatures below the onset of In desorption, it is difficult to avoid In accumulation and inclusions of crystalline In in the layer under In-rich conditions. © *2004 American Institute of Physics.* [DOI: 10.1063/1.1668318]

InN is currently attracting intense interest since a majority of recent reports have shown that its band gap is close to 0.7 eV[1–5] instead of 1.9–2 eV as believed previously.[6] Furthermore, high Hall mobilities have been reported of which some exceed 2000 $cm^2/V\,s$. Thus, InN exhibits promising properties for device applications. For example, in the optoelectronics field, the group-III nitride system might be used to fabricate light emitters covering the frequency range from infrared to ultraviolet. Other applications that have been suggested include low-cost solar cells,[7] high electron mobility transistors (HEMTs),[8] and color displays[9] based solely on III-nitrides. However, little has been reported on how the growth conditions affect the crystal quality and morphology of InN layers. The need for such an investigation is reflected by the fact that reported values regarding these properties are clearly inferior compared to both GaN and AlN.

It is well established that the growth of GaN(0001) and AlN(0001) under metal-stable conditions produces films which exhibit both a high crystal quality and a smooth surface. In addition, choosing a sufficiently high growth temperature results in a significant desorbing flux of the group-III element from the growth front, thus establishing a steady-state metal coverage while avoiding any accumulation and eventually droplet formation of either Ga or Al. However, it is not straightforward to adopt this growth mode for InN(0001) which dissociates at temperatures lower than those required for the desorption of In. Accumulation of In can thus be inhibited only by growth under slightly N-rich conditions, or by growth of InN(0001) as suggested by the recent work of Xu and Yoshikawa.[10]

In this letter, we present a study of the impact of different buffer layers and growth conditions on the properties of InN layers grown on 6H–SiC(0001) by plasma-assisted molecular beam epitaxy (PAMBE). The layers are characterized by various techniques, including reflection high-energy electron diffraction (RHEED), atomic force microscopy (AFM), x-ray diffraction (XRD), Hall measurements, as well as Raman, photoluminescence (PL) and optical transmission spectroscopy.

The InN films investigated here were grown on H_2 etched Si-face 6H–SiC(0001) substrates, resulting in cation-face GaN, AlN, and InN layers. A Ga flashoff procedure was performed in order to remove residual suboxides from the substrate surface prior to growth.[11] The substrate temperatures given in the following were calibrated by visual observation of the melting point of Al (660 °C) attached to the substrate. The PAMBE system employed was assembled by VTS-CreaTec, and is equipped with solid-source effusion cells for Ga, In, and Al, and a SVT radio-frequency plasma source operating at 300 W. The growth temperature for the GaN and AlN buffer layers was set to 760 °C and the N_2 flux was set to 1 sccm corresponding to metal-stable (bilayer) growth conditions in both cases. For the growth of the InN layer, the N_2 flux was set to 2 sccm. The growth rate of the InN layers was found to depend sensitively on the growth temperature.

The InN growth temperature was varied from 420 to 540 °C. All InN layers exhibited a wurtzite transmission RHEED pattern, reflecting a three-dimensional growth front. A superimposed reflection pattern was observed for layers grown under In-rich conditions. In droplets occurred on the surface of these latter layers. This excess In was removed by $HCl:H_2O(1:3)$ before further characterization took place. All samples are black in color and mirrorlike to the naked eye. The crystal quality was investigated by recording ω-scans across the InN(0002) reflection using a double-crystal x-ray diffractometer with wide open detector (rocking curves). The surface morphology was characterized by AFM operating in contact mode. Hall measurements in van der Pauw geometry using ohmic gold contacts were done to determine the carrier concentration and the Hall mobility. A 10 mW He–Ne laser emitting at 632.8 nm together with a liquid nitrogen cooled Ge photodetector was used for the PL and Raman measurements. The optical transmittance was measured by a Fourier-transform spectrometer at 300 K. The

[a]Electronic mail: ive@pdi-berlin.de

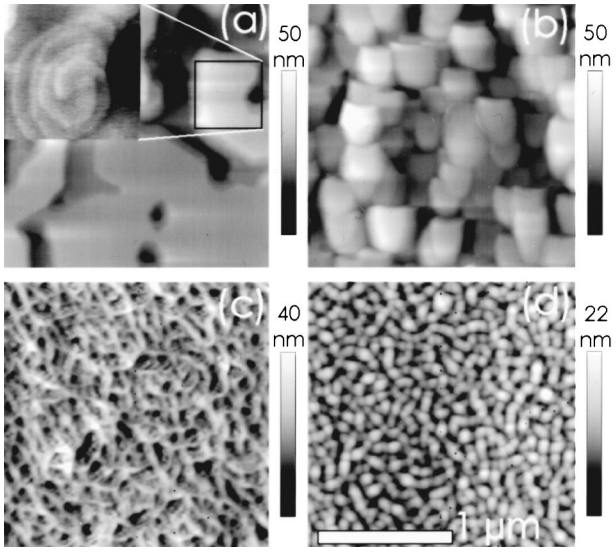

FIG. 1. AFM micrographs of InN layers (samples A–D) grown on a GaN buffer layer. The scale is indicated. The inset in (a) shows a 0.5×0.5 μm^2 closeup of a plateau.

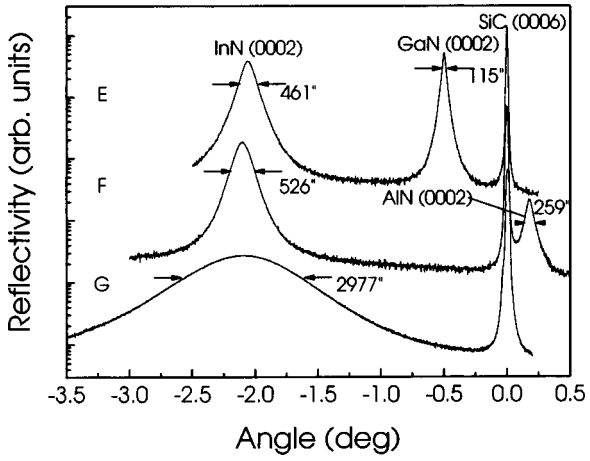

FIG. 2. X-ray rocking curves of InN layers grown at 460 °C either on a GaN (sample E) or AlN (sample F) buffer or directly on the SiC substrate (sample G). The profiles are vertically offset for clarity.

spectra were corrected for the spectral response of the system by normalizing them to those of bare SiC substrates.

Figure 1 shows AFM micrographs of InN layers grown on a GaN buffer layer at successively lower growth temperatures (Table I). Sample A [Fig. 1(a)] was grown at the highest temperature which resulted in effectively In-rich conditions whereas samples B–D [Figs. 1(b)–1(d)] were grown at lower temperatures and under N-rich conditions. There is a distinct change in the surface morphology with decreasing substrate temperature. Sample A exhibits a plateau-valley morphology with a very smooth surface on the plateaus, the latter of which approaches the morphology of the N-face InN films in Ref. 10 [note the inset in Fig. 1(a) that shows a monolayer growth spiral on a plateau]. The samples grown at lower temperatures and under N-rich conditions develop a spongelike morphology. Deep valleys, as present in sample A, are absent, as are atomic steps. Table I summarizes these and other measurement results. While the samples get progressively smoother with decreasing growth temperature, and in fact reach values for the rms roughness which compare favorably to those reported in the literature for In-face InN films,[8,9] the crystal quality, as measured by the FWHM of the InN(0002) reflection, is best at intermediate temperatures. Furthermore, both the background doping density and the Hall mobility are highest in sample A. Note that the Hall measurements do not distinguish between contributions from the bulk and a possible interfacial layer.

Figure 2 shows x-ray rocking curves from InN layers grown at 460 °C on GaN and AlN buffer layers and directly on SiC. The growth temperature for these samples was chosen to be in the intermediate range since this yields an acceptable compromise between crystal quality and surface morphology (Table I). The FWHM of the InN(0002) reflection for the two former samples is comparable and is close to the best values reported in the literature for In-face InN films.[10,12,13] In contrast, the sample nucleated directly on the SiC substrate exhibits a substantially broadened reflection. Note that we have made no attempt to optimize the nucleation of InN on SiC, as both GaN and AlN buffer layers lead to very satisfactory results regarding the layers' mosaicity. Furthermore, the FWHM of the E_2 (high) phonon mode observed at about 490 cm^{-1} in the Raman spectra of these samples are as narrow as 5.3–5.4 cm^{-1}, which is among the best values reported[5,12,14,15] and attests to the comparatively low disorder (heterogeneous strain) in these InN layers.

Figure 3 shows the optical transmission spectra of three of our thickest (450–500 nm) films, namely, samples E and F (Fig. 2) and sample H. From the measured transmittance T, we obtain a zeroth order approximation for the absorption coefficient $\alpha=-\ln(T)/d$. The inset shows $(\alpha E)^2$ vs E, which for parabolic bands should be a straight line and

TABLE I. Summary of the properties of all InN layers presented here. We list the InN layer thickness d as determined by scanning electron microscopy, the full width at half maximum (FWHM) of the InN(0002) reflection $\Delta\omega$ as well as the FWHM of the E_2 (high) phonon mode ΔE_2, the root-mean-square roughness rms, the carrier concentration n and the Hall mobility μ.

Sample	T_G (°C)	d (nm)	$\Delta\omega$ (arcsec)	ΔE_2 (cm^{-1})	rms (Å)	n (cm^{-3})	μ (cm^2/V s)
A	540	120	864	4.7	102	1.6×10^{20}	819
B	500	240	720		94		
C	460	260	540	6.4	79	5.6×10^{19}	441
D	420	500	1296	6.7	44	6.5×10^{19}	344
E	460	450	461	5.4	140	6.1×10^{19}	441
F	460	450	526	5.3	61	6.8×10^{19}	375
G	460	270	2977		52		
H	440	500	1383		52		

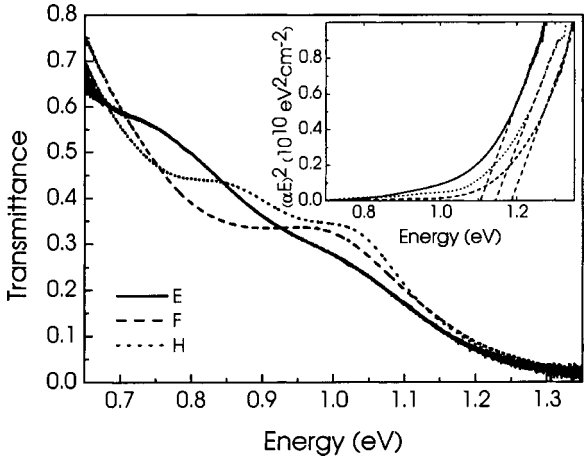

FIG. 3. Optical transmission spectra recorded at 300 K for three InN layers grown at 460 °C on GaN (samples E and H) or AlN (sample F) buffer layers. The fringes are due to thickness interferences. The inset shows the squared absorption coefficients vs. photon energy and linear extrapolations indicating the band gaps of the three samples.

whose extrapolation to zero is commonly taken to yield the band edge. For the three samples shown here, the estimated band gap thus lies in the range of 1.1–1.2 eV. These values are in good agreement with those found in Ref. 16 considering that the background carrier concentration of samples E and F is between 6×10^{19} and 7×10^{19}.

Finally, concerning emission from our samples, we found that all samples grown under N-rich conditions exhibit very weak PL signals or none at all. In contrast, the emission intensity of samples grown under In-rich conditions is considerably stronger. Figure 4 shows a PL spectrum of sample A at 6 K. The spectral position of the PL line is 0.78 eV and its FWHM is 82 meV. An additional measurement with an InSb detector confirmed the spectral position. The PL line rapidly diminishes in intensity with increasing temperature until it becomes undetectable at temperatures above 200 K. Considering the very high background doping (1.6×10^{20} cm^{-3}) and the high mobility of 819 cm^2/V s measured for this sample, we attribute this PL line to a band-to-band recombination of electrons from the bottom of the degenerate conduction band to photogenerated holes in the valence band. In this case, the PL peak energy is thus a more reliable indicator of the (renormalized) band gap than transmission measurements which are subject to a large Burstein–Moss shift induced by the high carrier density.

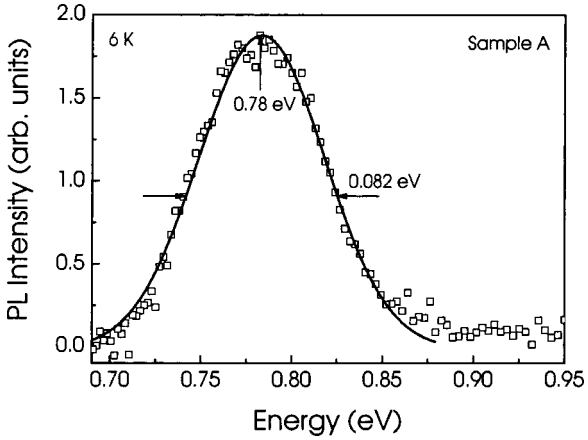

FIG. 4. PL spectrum at 6 K of sample A. The solid line is a Gaussian fit to the data for the determination of the FWHM and the peak energy position.

To conclude, our results are both qualitatively and quantitatively in exact agreement with the recent work of Xu and Yoshikawa.[10] The major obstacle in finding the most suitable growth conditions for In-face InN is the fact that the dissociation rate of InN is higher than the desorption rate of In. High temperature growth, as employed successfully for GaN and AlN, will thus inevitably result in accumulation of In. As a matter of fact, while we have observed that samples grown under In-rich conditions (e.g., sample A) have better electrical and optical properties than those grown under N-rich conditions, we also found, by XRD, that crystalline In inclusions tend to get incorporated in such layers. N-rich growth, on the other hand, generally results in poor surfaces, particularly at higher substrate temperatures. Exactly stoichiometric growth seems to be the only remedy of this problem, but requires an extremely precise control of the In and N fluxes.

The authors would like to thank Hans Peter Schönherr for technical assistance and Uwe Jahn for scanning electron microscopy.

[1] V. Yu. Davydov, A. A. Klochikhin, R. P. Seisyan, V. V. Emtsev, S. V. Ivanov, F. Bechstedt, J. Furthmüller, H. Harima, A. V. Mudryi, J. Aderhold, O. Semchinova, and J. Graul, Phys. Status Solidi B **229**, R1 (2002).
[2] V. Yu. Davydov, A. A. Klochikhin, V. V. Emtsev, S. V. Ivanov, V. V. Vekshin, F. Bechstedt, J. Furthmüller, H. Harima, A. V. Mudryi, A. Hashimoto, A. Yamamoto, J. Aderhold, J. Graul, and E. E. Haller, Phys. Status Solidi B **230**, R4 (2002).
[3] J. Wu, W. Walukiewicz, K. M. Yu, J. W. Ager III, E. E. Haller, H. Lu, W. J. Schaff, Y. Saito, and Y. Nanishi, Appl. Phys. Lett. **80**, 3967 (2002).
[4] J. Wu, W. Walukiewicz, K. M. Yu, J. W. Ager III, E. E. Haller, H. Lu, and W. J. Schaff, Appl. Phys. Lett. **80**, 4741 (2002).
[5] T. Matsuoka, H. Okamoto, M. Nakao, H. Harima, and E. Kurimoto, Appl. Phys. Lett. **81**, 1246 (2002).
[6] T. L. Tansley and C. P. Foley, J. Appl. Phys. **59**, 3241 (1986).
[7] W. Z. Shen, L. F. Jiang, H. F. Yang, and F. Y. Meng, Appl. Phys. Lett. **80**, 2063 (2002).
[8] H. Lu, W. J. Schaff, J. Hwang, H. Wu, G. Koley, and L. Eastman, Appl. Phys. Lett. **79**, 1489 (2001).
[9] M. Higashiwaki and T. Matsui, Jpn. J. Appl. Phys., Part 2 **41**, L540 (2002).
[10] K. Xu and A. Yoshikawa, Appl. Phys. Lett. **83**, 251 (2003).
[11] O. Brandt, R. Muralidharan, P. Waltereit, A. Thamm, A. Trampert, H. von Kiedrowski, and K. H. Ploog, Appl. Phys. Lett. **75**, 4019 (1999).
[12] V. V. Mamutin, V. A. Vekshin, V. Y. Davydov, V. V. Ratnikov, T. V. Shubina, S. V. Ivanov, P. S. Kopev, M. Karlsteen, U. Södervall, and M. Willander, Phys. Status Solidi A **176**, 247 (1999).
[13] V. V. Mamutin, V. A. Vekshin, V. Y. Davydov, V. V. Ratnikov, Y. A. Kudriavtsev, B. Y. Ber, V. V. Emtsev, and S. V. Ivanov, Phys. Status Solidi A **176**, 373 (1999).
[14] T. Inushima, V. V. Mamutin, V. A. Vekshin, S. V. Ivanov, T. Sakon, M. Motokawa, and S. Ohoya, J. Cryst. Growth **227/228**, 481 (2001).
[15] V. Y. Davydov, V. V. Emtsev, I. N. Goncharuk, A. N. Smirnov, V. D. Petrikov, V. V. Mamutin, V. A. Vekshin, S. V. Ivanov, M. B. Smirnov, and T. Inushima, Appl. Phys. Lett. **75**, 3297 (1999).
[16] J. Wu, W. Walukiewicz, W. Shan, K. M. Yu, J. W. Ager III, E. E. Haller, H. Lu, and W. J. Schaff, Phys. Rev. B **66**, 201403 (2002).